Toxicity and pharmacokinetic profile of SGM-101, a fluorescent anti-CEA chimeric antibody for fluorescence imaging of tumors in patients

Bérénice Framery, Marian Gutowski, Karen Dumas, Alexandre Evrard, Nathalie Muller, Vincent Dubois, Jérôme Quinonero, François Scherninski, André Pèlegrin, Françoise Cailler

Toxicology Reports 6 (2019) 409–415

Contents lists available at ScienceDirect

Toxicology Reports

journal homepage: www.elsevier.com/locate/toxrep

Toxicity and pharmacokinetic profile of SGM-101, a fluorescent anti-CEA chimeric antibody for fluorescence imaging of tumors in patients

Bérénice Framery[a], Marian Gutowski[b], Karen Dumas[a], Alexandre Evrard[b,c,d,e], Nathalie Muller[f], Vincent Dubois[f], Jérôme Quinonero[f], François Scherninski[g], André Pèlegrin[b,c,d,e,*], Françoise Cailler[a]

[a] SurgiMAb, 10 Parc Club du Millénaire, 1025 Avenue Henri Becquerel, 34000, Montpellier, France
[b] Institut régional du Cancer de Montpellier, ICM, Montpellier, F-34298, France
[c] IRCM, Institut de Recherche en Cancérologie de Montpellier, Montpellier, F-34298, France
[d] INSERM, U1194, Montpellier, F-34298, France
[e] Université de Montpellier, Montpellier, F-34298, France
[f] Leads to Development, 3-5 Impasse Reille, 75014, Paris, France
[g] Laboratoires Synth-Innove, 2bis rue Dupont de l'Eure, 75020, Paris, France

ARTICLE INFO

Keywords:
Carcinoembryonic antigen
Cancer
Fluorescence guided surgery
Near-infrared fluorochrome
Toxicity
Pharmacokinetics

ABSTRACT

The real-time improvement of the intraoperative discrimination between different tissue types (particularly between tumor and adjacent normal tissue) using intraoperative imaging represents a considerable advance for oncology surgeons. However, the development of imaging agents is much slower than that of drug therapies, although surgery represents one of the few curative treatments for many solid tumors. SGM-101 is a recently described, innovative antibody conjugate in which the near-infrared fluorochrome BM-104 is covalently linked to a chimeric monoclonal antibody against carcinoembryonic antigen (CEA). SGM-101 was developed with the goal of providing oncology surgeons with an intraoperative imaging tool that allows the visualization of CEA-overexpressing tumors. This antigen is overexpressed in a wide range of human carcinomas, such as colorectal, gastric, pancreatic, non-small cell lung and breast carcinomas. Here we characterized SGM-101 safety prior to its clinical testing for real-time cancer mapping by oncology surgeons. Safety pharmacology and toxicology studies were performed after intravenous injection of SGM-101 in Wistar rats and in Beagle dogs. SGM-101 metabolism and pharmacokinetics were analyzed in rats and mice. Finally, the potential toxicity of the BM-104 dye and SGM-101 cross-reactivity were assessed in a panel of 42 human tissues. Our pre-clinical toxicology, pharmacology and pharmacokinetic results demonstrated the absence of significant adverse effects of both SGM-101 and BM-104 at doses well above the anticipated maximal human exposure. Taken together, the results of the pharmacology, pharmacokinetic and toxicology studies support the development of SGM-101 as a potentially useful and safe tumor-specific imaging tool that might improve the complete tumor resection rate.

1. Introduction

Fluorescence guided surgery (FGS) is an expanding field with more and more clinical applications that could change the surgical oncology daily practice [1–3]. Thanks to dynamic research and development, several optical devices have been developed and marketed in recent years [4,5]. The main current limitation of FGS, particularly in oncology, is the limited choice of targeted contrast agents for the sensitive detection and precise delineation of tumor nodules in the surrounding normal tissue environment [2,6–8]. Indeed, survival is significantly different between patients who undergo total cancer resection and those with residual disease [9]. Moreover, the absence of tumor cells at the surgical margin is often considered as the strongest predictor of cancer recurrence or survival [10]. Currently, achieving negative margins relies on visual inspection, palpation, intraoperative ultrasound imaging and histopathological analysis of frozen tumor margin

Abbreviations: FGS, fluorescence guided surgery; NIR, near infra-red; ICG, indocyanine green; CEA, carcinoembryonic antigen; mAb, monoclonal antibody; GLP, Good Laboratory Practices; PK, pharmacokinetics; AUC, Area Under the Curve; MTD, maximum tolerated dose; MRT, Mean Residence Time; NOAEL, no observable adverse effect level (NOAEL); TMDD, target-mediated drug disposition

* Corresponding author.
E-mail address: andre.pelegrin@inserm.fr (A. Pèlegrin).

https://doi.org/10.1016/j.toxrep.2019.04.011
Received 8 November 2018; Received in revised form 18 April 2019; Accepted 28 April 2019
Available online 30 April 2019

sections [1]. However, with the development of minimally-invasive cancer surgery, surgeons more and more rely exclusively on vision for margin evaluation [1]. Peritoneal carcinomatosis is another potential major application of FGS. Indeed, in approximately 15% of patients with colorectal cancer, peritoneal carcinomatosis is already present at the time of diagnosis, and in 40% of patients, the disease is estimated to progress to peritoneal metastases after the initial diagnosis [11,12].

In their recent review [13] Boonstra et al. showed that most of the clinical studies on near infra-red (NIR) probes to visualize cancer investigated the use of non-targeted indocyanine green (ICG) to visualize lymph nodes in a wide range of tumor types. Only few trials evaluated targeted probes that are mostly based on therapeutic antibodies against angiogenic cells, which have been found to be suboptimal for tumor targeting [14–16]. On the other hand, several studies have shown that despite the presence of its soluble counterpart, carcinoembryonic antigen (CEA) is a particularly good target for tumor imaging [13,17–19]. This 200 kDa glycoprotein is overexpressed in most gastrointestinal tumors (including colorectal, pancreatic and gastric carcinoma) and in other epithelial tumors (ovary, uterus, thyroid, breast or lung cancer) [20,21]. In comparative studies, CEA is generally among the best markers for colorectal tumors and other cancer types with a high level of expression at the surface of tumor cells [13,17].

We recently described the development of SGM-101, an innovative antibody conjugate in which the BM-104 fluorochrome, which has an absorbance band centered at 700 nm, is coupled to SGM-Ch511, a chimeric monoclonal antibody (mAb) against CEA [22]. SGM-101 is suitable for diagnostic applications, such as the clear delineation of tumor masses within a normal environment, the detection of subclinical carcinomatosis in high-risk patients, and the assessment of residual disease for an adapted postoperative treatment. This should enable a more complete surgical resection of tumor lesions and subsequently greatly enhance the patient's prognosis.

Here, we describe the preclinical pharmacology and toxicology studies to evaluate SGM-101 and BM-104 safety and SGM-101 pharmacokinetics before its clinical testing.

2. Material and methods

2.1. Regulatory compliance

All animal experiments were performed in accordance with the French government guidelines and the Institut National de la Santé et de la Recherche Médicale (Inserm) regulations for experimental animal studies (agreement B34-172-27), with the approval by the relevant ethics committees. BM-104 mutagenic potential, SGM-101 tissue cross-reactivity, SGM-101 and BM-104 safety in rats and SGM-101 safety in dogs were assessed in compliance with the Good Laboratory Practices (GLP; Directive 2004/10/EC of the European Parliament and the Council of 11 February 2004).

2.2. Preparation of SGM-101

SGM-101 was prepared as previously described [22]. The anti-CEA chimeric SGM-ch511 mAb was produced on a large scale and then conjugated to BM-105 (the *N*-hydroxysuccinimide ester of the BM-104 dye). SGM-101 was prepared as a 1 mg/ml solution in PBS with 135 mM arginine.

2.3. Quantification of SGM-101 and BM-104 in plasma

SGM-101 plasma concentrations were determined using a quantitative ELISA method, as previously described [22]. The method was validated for the rat toxicokinetic study with a lower limit of quantification of 50.0 ng/mL. To evaluate the stability in human plasma of the covalent amide bonds between the SGM-Ch511 mAb and the BM-104 fluorochrome, human plasma samples from the Etablissement Français du Sang (batch #72132350989; O-) were incubated with 20 µg/mL SGM-101 at 37 °C for different times (from 30 min to 96 h). BM-104 plasma concentration was then determined by external standardization with a limit of detection of approximately 0.02 ppm (0.02 µg/mL).

2.4. Bacterial reverse mutation (Ames) test

BM-104 mutagenic potential was assessed by detection of mutations in five histidine-dependent *Salmonella typhimurium* strains [23]. Putative revertant cells (his− to his+) were detected on the basis of their ability to grow in the absence of histidine (required by the parent test strain) after incubation for 48 h with BM-104 (at concentrations from 50 to 5000 µg/plate) or with its potential metabolites that were produced by pre-incubation with a rat liver S9 fraction. Sodium azide (Sigma), 9-amino-acridine (Sigma), 2-nitrofluorene (Acros), mitomycin C (Sigma), 2-anthramine (Aldrich) and benzo(a)pyrene (Sigma) were used as positive controls for the different strains according to OECD No.471 and EC (440/2008) guidelines.

2.5. Tissue cross-reactivity of SGM-101

Characterization of the potential tissue cross-reactivity of SGM-101 was performed using a panel of 42 human frozen tissues (necropsies or surgical biopsies) from three unrelated donors (four serial sections of each tissue) (Cureline Inc., USA and Tissue Solution Ltd., UK), fresh human blood samples (Biopredic, France), and blood smears prepared by CiToxLAB, France. A biotin-labeled version of SGM-101 was used to allow the direct detection in immunohistochemistry experiments. After fixation and rehydration of the frozen sections, peroxidase activity was quenched with 3% hydrogen peroxide for at least 7 min. Incubation with the test (SGM-101) or control antibody for 1 h was followed by PBS washing, addition of the enzyme substrate from the ABC Vectastain kit for 30 min, PBS washes, incubation with the chromogen ImmPACT DAB (Vector Labs) for 8 min, water rinses, counterstaining and mounting. Immunostaining was performed at two concentrations of the test antibody (3.3 and 10 µg/mL) and at one concentration of the control antibody (10 µg/mL). Specific positive binding was graded according to the area and intensity of the staining as -: negative, 1: minimal, 2: slight, 3: moderate, 4: marked.

2.6. SGM-101 safety in rats

For toxicokinetic assessment, 6-week-old healthy male (n = 92) and female (n = 92) Wistar rats (Janvier, France) were randomized into four treatment groups: 0.9% NaCl (control group), and 5, 20 or 40 mg/kg SGM-101 (20 ml/kg for 4 h daily for 3 days for a total injected dose of SGM-101 of 15, 60 or 120 mg/kg). Each treatment group included a recovery group (5 + 1 males and 5 + 1 females), an interim group (10 + 1 males and 10 + 1 females) and a satellite group (6 males and 6 females). The supplementary animals (+1) were treated as the others and used to replace one of them if a technical problem with the catheter occured during treatment. Animals were all catheterized and blood samples and serum were collected at D0 + 5 h, D0 + 8 h, D1 + 5 h, D2 + 5 h, D3, D5, D12, D19 and D30 post-injection for the toxicokinetic study.

Morbidity, mortality, and evident signs of toxicity were monitored daily as part of a detailed clinical observation. Local tolerance was monitored daily from D0 to D7, then weekly. Body weight was monitored weekly. Food and drink intake were recorded at least once per week. Body temperature was measured 2 h after each injection at D0, D1 and D2 (and D3 during the functional observational battery (FOB) protocol). Ophthalmoscopy was performed before the first treatment, at D3 and during the last week of the study. Blood was collected at D6 (interim animals) and D30 (recovery animals) for blood count and chemistry testing, and urine at D6 (recovery animals). Animals were sacrificed and macroscopic autopsy was performed at D6 (interim

animals) and D30 (recovery animals). Organs were collected and preserved; histopathology analysis was performed in interim animals (control and 40 mg/kg SGM-101 group). Blood smear analysis was performed using blood samples collected at D6 (interim males and females) and D30 (recovery animals of the control and 40 mg/kg SGM-101 group).

2.7. BM-104 safety in rats

Healthy Wistar rats were randomized into four treatment groups that received one intravenous injection of vehicle (NaCl 0.9%), 0.85 mg/kg BM-104, 1.7 mg/kg BM-104 or 3.4 mg/kg BM-104. Each treatment group included a recovery group (10 males and 10 females) and an interim group (20 males and 20 females). Toxicity was evaluated by monitoring the animals for 28 days. Morbidity, mortality, and evident signs of toxicity were monitored daily as part of a detailed clinical observation. Local tolerance was monitored daily from D0 to D7, then weekly. Body weight was monitored weekly, and food and drink intake were recorded twice a week. Body temperature was measured 2 h after injection at D0. Ophthalmoscopy was performed 7 days before injection (D-7), D1 (interim and recovery animals) and D27 (recovery animals). Blood was collected at D4 (interim animals) and D28 (recovery animals), and urine at D4 from recovery animals. Animals were sacrificed and macroscopic autopsy was performed at D4 (interim animals) and D28 (recovery groups). Histopathology analysis was performed on interim animals of the control and 3.4 mg/kg BM-104 group. Blood smear analysis was performed using blood samples collected at D4 from the interim control and 3.4 mg/kg BM-104 groups.

2.8. SGM-101 safety in dogs

Six beagle dogs (three males, three females) (Marshall Farms) were equipped with telemetric transmitters (Data Sciences International, PA-C10). They were assigned to a single group that received first one intravenous infusion of 5 mg/kg SGM-101 during 4 h and then, after a wash-out period of at least 10 days, another infusion of 20 mg/kg SGM-101 for 4 h. The test item was administered as a solution in vehicle (PBS with 135 mM arginine). Cardiovascular (ECG, blood pressure) and respiratory recordings were performed on conscious animals using external telemetry monitoring. Cardiovascular parameters were assessed before the administration of each dose and at 0.25, 0.5, 1, 2, 3, 4, 6, 8, 12, 16, 20 and 24 h after the beginning of the infusion. ECG recordings were reviewed to evaluate the occurrence of arrhythmia at the analysis time points. Respiratory parameters were evaluated in hammocks before dose administration and at 0.25, 0.5, 1, 2, 3, 4 (end of the infusion period) and 5 h, and then after the animals' return to their pens at 6 h post-infusion initiation. Morbidity, mortality, clinical signs, body weight, food consumption, and ophthalmoscopic parameters were assessed as well as blood count and chemistry.

2.9. ^{125}I-SGM-101 biodistribution in mice

^{125}I-SGM-101 was prepared as described with 2.5μCi ^{125}I/μg [22]. After intravenous injection of 30 or 60 μg of ^{125}I-SGM-101 in transgenic mice that express human CEA [24] (produced by Charles River) or in the parental strain (C57BL/6) (Janvier), animals were sacrificed at different time points. At each time point and up to 10 days post-injection, 3 males and 3 females from each strain were sacrificed and radioactivity was measured in selected organs, and in plasma using a gamma-well counter. ^{125}I-SGM-101 plasma concentration at each time point was back-calculated from the measured radioactivity levels and used to determine key pharmacokinetic parameters. All organs were weighed and their radioactivity (^{125}I) measured using a gamma counter (Cobra II; Packard). Results were expressed as percentage of the injected dose (ID) per gram of tissue (% ID/g). For the evaluation of the total radioactivity level in mice, the level of radioactivity in whole live animals who received [^{125}I]-SGM-101 was quantified by placing the animal in a CRC-15 W radioisotope dose calibrator (Capintec, Inc., Pittsburgh, USA) for instant quantification.

2.10. Pharmacokinetic analysis

Data from the pharmacokinetics (PK) and biodistribution experiments were analyzed by using PK solver, an Excel add-in described in [25]. The PK parameters Area Under the Curve (AUC), Mean Residence Time (MRT) and clearance were estimated using a non-compartmental analysis. The AUC from the zero time and up to the last time t (AUC_{0-t}) and the area under the first moment curve from 0 to the last time t ($AUMC_{0-t}$) were calculated using the linear trapezoidal method and estimation of the terminal elimination slope by linear regression. For biodistribution experiments in mice, the decrease of the whole amount of radioactivity at the animal level was considered and expressed as μg after injection of an equivalent single dose of 30 μg of antibody.

2.11. Blood and urine testing

Hematology parameters were measured on whole blood. For biochemistry analyses, plasma was prepared according to conventional procedures and aliquoted in two parts: one aliquot was assayed extemporaneously and the other aliquot were stored either at + 4 °C or at − 20 °C until analysis.

Urine was collected by placing rats during 12 h–18 h in individual metabolism cages and fasting them during urine collection.Volume was measured and appearance observed: sticky or not, color (white, pale yellow, straw colored, yellow-orange colored, red…), translucent, opaque or creamy.

The pH of urine and presence of proteins, glucose and blood cells were checked by Medi-Test Combi 10® VET urine strips (Macherey-Nagel, Germany).The pH test is based on a dual colour indicator that can cover the entire range of urinary pH.Testing for protein is based on the phenomenon called the "Protein Error of Indicators" (ability of protein to alter the colour of some acid-base indicators without altering the pH).

Sodium, potassium, creatinin and urea (and total proteins and glucose if detected by urine strips) were quantified in urine samples using the qualified Cobas Mira biochemistry analyzer (4 M, France). These parameters allow calculating osmolality using formula: Urine osmolality = 2 (Na + K) + glucose + urea.

2.12. Ophtalmoscopy

Ophthalmological (Dogs) examinations were performed on all animals before the beginning of the treatment period, after each dosing at the end of the infusion period and on completion of the treatment period.

Pupillary light and blink reflexes were evaluated first. The pupils of the animals were then dilated with tropicamide (Mydriaticum®, Laboratoires Théa, Clermont-Ferrand, France), and the appendages, optic media and fundus were examined by indirect ophthalmoscopy. The anterior segment and the lens were examined using a slit-lamp biomicroscope.

3. Results

3.1. SGM-101 stability in human plasma

SGM-101 stability in human plasma was evaluated by incubating human plasma sample with 20 μg/mL SGM-101 at 37 °C and then quantifying the amount of free BM-104. Whatever the incubation time, the level of free BM-104 remained below the limit of detection of the method (0.02 ppm). It was therefore concluded that BM-104 is not significantly released from the conjugate in these conditions.

3.2. BM-104 mutagenic potential

BM-104 mutagenic potential was assessed using the Ames test. Incubation with BM-104 (from 50 to 5000 µg/plate) or its metabolites did not induce the growth of a significant number of revertants, differently from the positive controls. Therefore, BM-104 was not considered mutagenic for these strains.

3.3. SGM-101 cross-reactivity

Analysis of SGM-101 binding in blood smears and in a panel of 42 human frozen tissues from three unrelated individuals showed specific signals in samples from one donor, when using 3.3 and/or 10 µg/mL of SGM-101. The SGM-101 signal was limited to the epithelial components, primarily at the apical cell border or luminal side, of the digestive tract and few other tissues. As all SGM-101-positive tissues are known to express CEA to some extent, the staining pattern was considered to represent the on-target binding of SGM-101.

3.4. SGM-101 and BM-104 safety and pharmacokinetic studies in rats

SGM-101 intravenous injection (at 5, 20 and 40 mg/kg/day by daily infusion for 3 days) did not affect the rats' body weight and body temperature, and had no significant effect on organ weight. Post-mortem macroscopic examination showed the presence of various types of liver discoloration in 1/10 males and 7/10 females that received the highest dose, without histological changes. Given the nature of the tested molecules, these discolorations are probably related to the treatment, but they were not considered as adverse events. Moreover, histological analysis of the organs collected at D6 did not suggest any toxic effect of SGM-101. Indeed, it was well-tolerated at the injection site and no abnormality was observed in lymphoid organs.

The behavior of rats in all the experimental groups was monitored at D3 and during the week before sacrifice following the FOB protocol (home cage observations, handling observations, open-field observations, and measurement of reflexes and physiological parameters). No difference was observed between rats treated with vehicle or with SGM-101.

SGM-101 maximum tolerated dose (MTD) was not reached and the no observable adverse effect level (NOAEL) was considered to be at least 40 mg/kg per day for 3 days.

SGM-101 content was quantified in plasma to calculate its main PK parameters (Table 1). SGM-101 plasma levels increased almost proportionally with the SGM-101 dose, then rapidly decreased 24 h after the last SGM-101 injection, and could still be detected at low levels at D30 (720 h post-injection) (Fig. 1). SGM-101 exposure was slightly higher in males than females at the highest dose. However, the main PK parameters were comparable between sexes (Table 1). SGM-101 PK was nearly linear (proportionality between dose and AUC) from 15 to 120 µg/kg, consistent with the absence of the antibody target in rats and the absence of target-mediated drug disposition (TMDD). SGM-101 concentration decrease as a function of time was comparable between sexes and showed a very slight inter-individual variability (Fig. 1). A semi-log representation of these data showed a bi-phasic elimination of SGM-101, as often described for other IgG1 (data not shown).

Table 1
SGM-101 pharmacokinetic parameters in healthy Wistar rats.

Injected dose (mg/kg)	Sex	C53h (µg/ml)	AUC0-$_\infty$ (µg.h.ml^{-1})	MRT (h)	Clearance (ml.h^{-1}.kg^{-1}.10^{9})
15	Male	133	22 086	186	679
	Female	149	23 901	229	627
60	Male	558	68 217	147	879
	Female	512	93 980	233	638
120	Male	909	151 892	178	790
	Female	675	104 265	146	1151

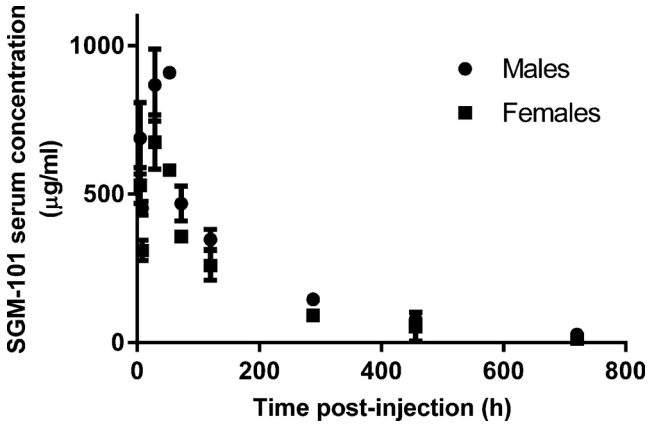

Fig. 1. SGM-101 plasma concentration in rats as a function of time after intravenous infusion of 120 mg/kg SGM-101 in total (one 4h-infusion of 40 mg/kg SGM-101/day for 3 days).

Finally, acute intravenous administration of BM-104 in rats at doses up to 3.4 mg/kg (which corresponds to 140 times the intended clinical dose) was well tolerated and did not induce any evident sign of toxicity. Therefore, the BM-104 NOAEL was considered to be 3.4 mg/kg in rats.

3.5. SGM-101 safety study in dogs

Then, the potential toxicity of SGM-101 and its effects on cardiovascular and respiratory functions were evaluated by telemetry in Beagle dogs after intravenous infusion of SGM-101 (5 mg/kg as the intermediate dose-level and 20 mg/kg as the high dose-level) for 4 h. Besides transient, spontaneously resolving signs of an anaphylactoid or anaphylactic reaction at the highest dose-level, no other significant adverse effect of SGM-101 was reported. The NOAEL of SGM-101 was considered to be 5 mg/kg. Specifically, no statistically significant change in heart rate, arterial blood pressure (systolic, diastolic and mean arterial blood pressures) or electrophysiological parameters was observed after SGM-101 infusion (both concentrations) compared with vehicle. No alterations in respiratory parameters (respiratory rate, tidal and minute volumes) were reported. Food consumption and body weight were not affected whatever the tested dose. No ophthalmologic alteration was observed. No clinical sign was reported after infusion of 5 mg/kg SGM-101. Conversely, with 20 mg/kg SGM-101, erythema, swelling of the ears, and/or soft feces were observed in 3/6 animals during the infusion. These signs were associated with a transient decrease of the arterial blood pressure and increase of the heart rate in one animal. These symptoms could have been caused by an anaphylactoid reaction to SGM-101, and they resolved spontaneously shortly after the end of the infusion (from 45 min to 24 h after beginning of the infusion whose duration was 4 h; the longest one was an erythema for 1 animal; the others ones were resolved before the end of the infusion). Reduced lymphocyte counts were observed after infusion with vehicle or SGM-101 (both doses), but normal levels were restored two days after treatment.

3.6. Local tolerance in rats and dogs

The local tolerance to intravenous BM-104 and SGM-101 administration was systematically evaluated (daily during the first week post-infusion and then weekly) within the scope of the toxicology studies performed in rats and dogs. There was no significant treatment-related macroscopic or microscopic finding.

Table 2
SGM-101 exposure parameters in transgenic mice that express human CEA and in wild type controls.

Mice	Sex	AUC0-$_\infty$ (μg.h)	MRT (h)
Transgenic	Male	4848	223
	Female	5049	198
Wild type	Male	6347	271
	Female	5450	217

3.7. Biodistribution in normal and transgenic mice

Biodistribution studies were performed using ^{125}I-SGM-101 since this iodine labeling gives a more realistic picture of biodistribution than those used for imaging purposes, such as ^{111}In (when SGM-101 is degraded, ^{125}I and BM104 are eliminated) [26]. The possible influence of CEA expression on SGM-101 PK and tissue distribution was assessed by injecting ^{125}I-SGM-101 in transgenic mice that express human CEA [24] and in the parental strain (C57BL/6). The overall exposure was evaluated by measuring the radioactivity decay followed by a non-compartmental analysis. The MRT and AUC were slightly reduced (from 10 to 20%) in CEA-expressing animals (Table 2), suggesting a higher clearance of SGM-101 in the presence of the antigen, consistent with a TMDD phenomenon. As previously observed in rats, exposure was slightly different between sexes in the parental strain. Conversely, the levels of radioactivity found in the organs were not different between males and females, as well as between transgenic and wild type animals. This was expected because CEA expression in this transgenic model is exclusively apical, and the antigen is not accessible to circulating SGM-101. The temporal changes of the proportion of the injected dose found per gram of tissue in each organ is detailed in Table 3 (mean values for all transgenic and wild type males and females taken as a single group). After 10 days, less than 5% of the initial dose could be detected (less than 10% in blood).

4. Discussion

We recently described SGM-101, a mAb-fluorochrome conjugate that targets CEA. Its optical characteristics and its stability make of it an excellent candidate for real-time intraoperative tumor imaging, and it binds efficiently to human CEA-expressing cells *in vivo* in several mouse models [22].

For many years, CEA has been considered a promising target for monoclonal antibodies to be used in radio-immunodiagnostic and radio-immunotherapy. Therefore, extensive data on a wide range of anti-CEA antibodies from more than hundred clinical studies are available, considerably reducing the risk associated with the use of SGM-101 [27–29]. However, none of the animal species commonly used in toxicology studies (rodents, dogs, non-human primates) expresses CEA. Therefore, there is no relevant species for the evaluation of the toxicity profile of anti-CEA antibodies or conjugates, such as SGM-101. The use of transgenic mice expressing human CEA [24] is not considered appropriate for toxicology studies because the effects associated with the presence of the transgene and/or its expression have not been appropriately characterized.

Therefore, the preclinical toxicological evaluation of SGM-101 was restricted to the study of the effects of its acute intravenous administration in rats. This is consistent with the intended clinical use because patients will receive a single intravenous administration prior to surgery. The dose administered in rats was approximately 85 times the maximum anticipated clinical dose. The safety pharmacology study in

Table 3
Percentage of ^{125}I-SGM-101 injected dose per gram of tissue in different organs and at different time points after injection in all mice (transgenic and wild type).

	Time								
Organ	0	2h	8h	24h	48h	72h	96h	7 days	10 days
Blood	53	39	26	19	17	14	14	11	≤10
Lung	18	15	11	8	8	6	7		
Uterus	2	9	12	7	9	7	7		
Spleen	5	15	10	7	6				
Heart	15	13	8	6	6				
Ovaries	4	9	10	6	7				
Liver	13	11	8	5	5				
Kidney	12	12	9	6					
Bladder	2	5	9	6					
Others									

Grey cells: values < 5%.
Others include skin, stomach, small intestine, colon, testis, tongue, pancreas, prostate, esophagus, skeletal muscle, bone, brain, eyes, and carcass.

Beagle dogs evaluated the cardiovascular and respiratory functions after SGM-101 administration (at approximately 45 times the maximal intended clinical dose) and also included the analysis of several toxicology endpoints to collect additional data in a second animal species.

No significant adverse reaction/toxicity was observed, with the exception of the occurrence of an infusion (likely anaphylactoid-type) reaction in some dogs that resolved spontaneously. Such infusion reactions are common when using biological medicinal products, particularly antibodies, and are usually clinically manageable [30–32]. If this is considered as an adverse reaction, the NOAEL in the dog can be estimated at 5 mg/kg, or 100 mg/m^2. This suggests that Beagle dogs are more sensitive than rats (NOAEL = 40 mg/kg or 240 mg/m^2).

GLP-compliant safety pharmacology studies demonstrated that intravenous administration of SGM-101 did not lead to any adverse events in the central and peripheral nervous systems in Wistar rats, or on the cardiovascular and respiratory functions in Beagle dogs at dose levels of up to 40 mg/kg (240 mg/m2) and 20 mg/kg (400 mg/m2), respectively.

A tissue cross-reactivity study was carried to detect potential unintentional reactivity towards non-targeted human tissues. All the tissues where staining was observed are known to express CEA to some extent [20]. Therefore the observed SGM-101 staining pattern was considered to represent on-target binding.

In vitro stability studies in human plasma at 37 °C confirmed the stability of the amide bonds linking the BM-104 fluorochrome to the antibody. Moreover, BM-104 toxicity assessment in Wistar rats did not find any sign of toxicity at 3.4 mg/kg (140-fold the maximal anticipated clinical exposure), and BM-104 was non-mutagenic in the Ames test.

In vivo studies conducted in a human CEA-expressing mouse model showed similar pharmacokinetic profiles as in the wild type strain. CEA expression in this transgenic model is exclusively apical, and the antigen is not accessible to circulating SGM-101. Tissue distribution also was comparable in transgenic and in wild type animals. Moreover, at day 10 after injection only 10% of the injected dose of SGM-101 could be detected in blood (Table 3). SGM-101 is also rapidly eliminated in immunosuppressed mice bearing human intraperitoneal CEA-overexpressing tumors and in normal Swiss mice [22]. The toxicokinetic evaluation performed in Wistar rats after intravenous injection of 5, 20 or 40 mg/kg/day showed that plasma SGM-101 levels increased with the SGM-101 injected dose in an almost proportional manner.

The results of these toxicology studies helped to determine the starting dose of SGM-101 used in clinical trials (NCT02784028, NCT02973672). The NOAEL in the dog was evaluated at 5 mg/kg, or 100 mg/m^2, and in the rat at 40 mg/kg or 240 mg/m^2. Therefore, a starting dose of 5 mg (3 mg/m^2 for a 1.7 m^2 patient) was chosen, providing a significant, 33-fold safety margin relative to the NOAEL in the dog. The safety margin was still 11-fold for the highest anticipated dose (15 mg or 9 mg/m2). Being over the 10 fold excess typically recommended by health authorities prior to a first injection to a human subject, it was considered to be sufficient for this type of product. Indeed, an evaluation of the safety data was performed for the eighteen patients included in the NCT02784028 trial (patients with peritoneal carcinomatosis from CEA-overexpressing digestive cancers) and for the 46 ones included in the NCT02973672 trial (16 patients with primary and 30 patients with recurrent colorectal cancer). There appeared to be no safety concerns associated with iv administration of SGM-101 at doses up to 15 mg infused over 30 min [33,34].

Near-infrared cameras that can visualize SGM-101 with a sensitivity adapted to cancer detection are available and some have been cleared by FDA and/or the European community [35]. Some multispectral models even offer the possibility to work concomitantly with two or more fluorophores with distinct excitation and emission wavelengths. The optical characteristics of SGM-101, described recently by Gutowski, Framery et al. [22], correspond to what is expected for use in FGS. Moreover, with emission and excitations wavelengths close to 700 nm, SGM-101 is perfectly adapted to be used with ICG for precise detection of tumor tissue and reconstruction purposes, respectively. The current clinical trials will assess SGM-101 efficacy for the detection of small tumor nodules of digestive origin and should allow choosing the best dose for digestive tumor detection.

Disclosures

FC, BF, KD are employed by SurgiMAb that owns the SMG-101 conjugate and SurgiMAb stockholders.

FC, AP, MG are SurgiMAb founders and stockholders.

FS is CEO of Synth:Innove that developed and patented the BM-104 dye.

Transparency document

The Transparency document associated with this article can be found in the online version.

Acknowledgment

This research was supported by SurgiMAb.

References

[1] K.E. Tipirneni, J.M. Warram, L.S. Moore, et al., Oncologic procedures amenable to fluorescence-guided surgery, Ann. Surg. (2016), https://doi.org/10.1097/SLA.0000000000002127.
[2] A.L. Vahrmeijer, M. Hutteman, J.R. van der Vorst, et al., Image-guided cancer surgery using near-infrared fluorescence, Nat. Rev. Clin. Oncol. 10 (2013) 507–518, https://doi.org/10.1038/nrclinonc.2013.123.
[3] J.D. Predina, D. Fedor, A.D. Newton, et al., Intraoperative molecular imaging: the surgical oncologist's north star, Ann. Surg. 266 (2017) e42–e44, https://doi.org/10.1097/SLA.0000000000002247.
[4] S. Keereweer, P.B.A.A. Van Driel, T.J.A. Snoeks, et al., Optical image-guided cancer surgery: challenges and limitations, Clin. Cancer Res. 19 (2013) 3745–3754, https://doi.org/10.1158/1078-0432.CCR-12-3598.
[5] A.V. DSouza, H. Lin, E.R. Henderson, et al., Review of fluorescence guided surgery systems: identification of key performance capabilities beyond indocyanine green imaging, J. Biomed. Opt. 21 (2016) 80901, https://doi.org/10.1117/1.JBO.21.8.080901.
[6] Q.T. Nguyen, R.Y. Tsien, Fluorescence-guided surgery with live molecular navigation–a new cutting edge, Nat. Rev. Cancer 13 (2013) 653–662, https://doi.org/10.1038/nrc3566.
[7] E.L. Rosenthal, J.M. Warram, E. de Boer, et al., Successful translation of fluorescence navigation during oncologic surgery: a consensus report, J. Nucl. Med. 57 (2016) 144–150, https://doi.org/10.2967/jnumed.115.158915.
[8] S. Gioux, H.S. Choi, J.V. Frangioni, Image-guided surgery using invisible near-infrared light: fundamentals of clinical translation, Mol. Imaging 9 (2010) 237–255.
[9] J. Parrish-Novak, E.C. Holland, J.M. Olson, Image guided tumor resection, Cancer J. Sudbury Mass 21 (2015) 206, https://doi.org/10.1097/PPO.0000000000000113.
[10] Q.T. Nguyen, R.Y. Tsien, Fluorescence-guided surgery with live molecular navigation — a new cutting edge, Nat. Rev. Cancer 13 (2013) 653–662, https://doi.org/10.1038/nrc3566.
[11] M.J. Koppe, O.C. Boerman, W.J.G. Oyen, R.P. Bleichrodt, Peritoneal carcinomatosis of colorectal origin: incidence and current treatment strategies, Ann. Surg. 243 (2006) 212–222, https://doi.org/10.1097/01.sla.0000197702.46394.16.
[12] T.C. Chua, J. Esquivel, J.O.W. Pelz, D.L. Morris, Summary of current therapeutic options for peritoneal metastases from colorectal cancer, J. Surg. Oncol. 107 (2013) 566–573, https://doi.org/10.1002/jso.23189.
[13] M.C. Boonstra, S.W.L. de Geus, H.A.J.M. Prevoo, et al., Selecting targets for tumor imaging: an overview of cancer-associated membrane proteins, Biomark. Cancer 8 (2016) 119–133, https://doi.org/10.4137/BIC.S38542.
[14] C.H. Heath, N.L. Deep, L.N. Beck, et al., Use of Panitumumab-IRDye800 to image cutaneous head and neck Cancer in mice. otolaryngol–head neck surg off, J. Am. Acad. Otolaryngol.-Head Neck. Surg. (2013), https://doi.org/10.1177/0194599813482290.
[15] M.L. Korb, Y.E. Hartman, J. Kovar, et al., Use of monoclonal antibody-IRDye800CW bioconjugates in the resection of breast cancer, J. Surg. Res. 188 (2014) 119–128, https://doi.org/10.1016/j.jss.2013.11.1089.
[16] A.G.T. Terwisscha van Scheltinga, G.M. van Dam, W.B. Nagengast, et al., Intraoperative near-infrared fluorescence tumor imaging with vascular endothelial growth factor and human epidermal growth factor receptor 2 targeting antibodies, J. Nucl. Med. 52 (2011) 1778–1785, https://doi.org/10.2967/jnumed.111.092833.
[17] J.P. Tiernan, S.L. Perry, E.T. Verghese, et al., Carcinoembryonic antigen is the preferred biomarker for in vivo colorectal cancer targeting, Br. J. Cancer 108 (2013) 662–667, https://doi.org/10.1038/bjc.2012.605.
[18] C.E. Hoogstins, B. Weixler, L.S. Boogerd, et al., In search for optimal targets for intraoperative fluorescence imaging of peritoneal metastasis from colorectal cancer,

Biomark. Cancer 9 (2017), https://doi.org/10.1177/1179299X17728254 1179299X17728254.
[19] T.K. Nikolouzakis, L. Vassilopoulou, P. Fragkiadaki, et al., Improving diagnosis, prognosis and prediction by using biomarkers in CRC patients (Review), Oncol. Rep. 39 (2018) 2455–2472, https://doi.org/10.3892/or.2018.6330.
[20] S. Hammarström, The carcinoembryonic antigen (CEA) family: structures, suggested functions and expression in normal and malignant tissues, Semin. Cancer Biol. 9 (1999) 67–81, https://doi.org/10.1006/scbi.1998.0119.
[21] S. Saadatmand, E.M. de Kruijf, A. Sajet, et al., Expression of cell adhesion molecules and prognosis in breast cancer, Br. J. Surg. 100 (2013) 252–260, https://doi.org/10.1002/bjs.8980.
[22] M. Gutowski, B. Framery, M.C. Boonstra, et al., SGM-101: An innovative near-infrared dye-antibody conjugate that targets CEA for fluorescence-guided surgery, Surg. Oncol. (2019).
[23] B.K. Soni, J.P. Langan, Mutagenicity and genotoxicity of ClearTaste, Toxicol. Rep. 5 (2018) 196–206, https://doi.org/10.1016/j.toxrep.2017.12.015.
[24] P. Clarke, J. Mann, J.F. Simpson, et al., Mice transgenic for human carcinoembryonic antigen as a model for immunotherapy, Cancer Res. 58 (1998) 1469–1477 https://doi.org/9537250.
[25] Y. Zhang, M. Huo, J. Zhou, S. Xie, PKSolver: an add-in program for pharmacokinetic and pharmacodynamic data analysis in Microsoft Excel, Comput. Methods Programs Biomed. 99 (2010) 306–314, https://doi.org/10.1016/j.cmpb.2010.01.007.
[26] J.P. Mach, A. Pèlegrin, F. Buchegger, Imaging and therapy with monoclonal antibodies in non-hematopoietic tumors, Curr. Opin. Immunol. 3 (1991) 685–693.
[27] D.M. Goldenberg, R.M. Sharkey, G. Paganelli, et al., Antibody pretargeting advances cancer radioimmunodetection and radioimmunotherapy, J. Clin. Oncol. 24 (2006) 823–834, https://doi.org/10.1200/JCO.2005.03.8471.
[28] D.M. Goldenberg, F. DeLand, E. Kim, et al., Use of radiolabeled antibodies to carcinoembryonic antigen for the detection and localization of diverse cancers by external photoscanning, N. Engl. J. Med. 298 (1978) 1384–1386, https://doi.org/10.1056/NEJM197806222982503.
[29] J.P. Mach, S. Carrel, M. Forni, et al., Tumor localization of radiolabeled antibodies against carcinoembryonic antigen in patients with carcinoma: a critical evaluation, N. Engl. J. Med. 303 (1980) 5–10, https://doi.org/10.1056/NEJM198007033030102.
[30] S.P. Kang, M.W. Saif, Infusion-related and hypersensitivity reactions of monoclonal antibodies used to treat colorectal cancer–identification, prevention, and management, J. Support. Oncol. 5 (2007) 451–457.
[31] C.H. Chung, Managing premedications and the risk for reactions to infusional monoclonal antibody therapy, Oncologist 13 (2008) 725–732, https://doi.org/10.1634/theoncologist.2008-0012.
[32] B.A. Baldo, Adverse events to monoclonal antibodies used for cancer therapy: focus on hypersensitivity responses, Oncoimmunology 2 (2013) e26333, , https://doi.org/10.4161/onci.26333.
[33] L.S.F. Boogerd, C.E.S. Hoogstins, D.P. Schaap, et al., Safety and effectiveness of SGM-101, a fluorescent antibody targeting carcinoembryonic antigen, for intraoperative detection of colorectal cancer: a dose-escalation pilot study, Lancet Gastroenterol. Hepatol. (2018), https://doi.org/10.1016/S2468-1253(17)30395-3.
[34] C.E.S. Hoogstins, L.S.F. Boogerd, B.G. Sibinga Mulder, et al., Image-guided surgery in patients with pancreatic cancer: first results of a clinical trial using SGM-101, a novel carcinoembryonic antigen-targeting, near-infrared fluorescent agent, Ann. Surg. Oncol. (2018), https://doi.org/10.1245/s10434-018-6655-7.
[35] R.R. Zhang, A.B. Schroeder, J.J. Grudzinski, et al., Beyond the margins: real-time detection of cancer using targeted fluorophores, Nat. Rev. Clin. Oncol. 14 (2017) 347–364, https://doi.org/10.1038/nrclinonc.2016.212.